Published by Institute of Physics Publishing for SISSA

Received: *December 17, 2006*
Revised: *January 17, 2007*
Accepted: *January 18, 2007*
Published: *February 7, 2007*

QCD with one compact spatial dimension

Thomas DeGrand and Roland Hoffmann

Department of Physics, University of Colorado,
Boulder, CO 80309 U.S.A.
E-mail: degrand@pizero.colorado.edu, hoffmann@pizero.colorado.edu

Abstract: The realization of global symmetries can depend on the geometry of the underlying space. In particular, compactification can lead to spontaneous breaking of such symmetries. Four-dimensional QCD with fundamental representation fermions embedded in a space with one compact spatial dimension has a critical length, at which the theory undergoes a phase transition and develops a ground state that is no longer charge conjugation invariant. We show this behavior with simulations of three color, four flavor QCD. We use unrooted staggered fermion at two values of the lattice spacing and several quark masses. We discuss the dependence of the transition on the dynamical fermion mass as well as its connection to the finite temperature and chiral phase transitions.

Keywords: Lattice Gauge Field Theories, Global Symmetries, Spontaneous Symmetry Breaking.

JHEP02(2007)022

Contents

JHEP02(2007)022

1. Introduction

1.1 Motivation

When field theories are defined on spaces with one or more compact directions, the sizes of the compact dimensions can influence the existence and location of phase transitions. The most familiar example of this behavior is the use of a compact temporal dimension to study a field theory at finite temperature. In this paper we describe such a situation, which occurs in ordinary QCD (with dynamical fermions): a sufficiently small compact spatial dimension induces a transition into a phase in which charge conjugation is spontaneously broken. The existence of this new phase, and of the length scale which characterizes the transition, depend on the choice of periodic fermionic boundary conditions in the compact dimension(s).

The effect we describe is similar to the deconfinement transition in QCD with dynamical fermions. The action of SU(N) pure gauge theories is invariant under gauge transformations which are periodic up to multiplication by the center of the gauge group, $Z(N)$ for SU(N). These theories have an order parameter, the Polyakov loop or Wilson line, which is sensitive to such transformations. The low temperature phase of the theory is one in which the vacuum expectation value of the order parameter vanishes. In the high temperature phase, the order parameter spontaneously magnetizes along one of the directions of the center of the gauge group, signaling deconfinement. Now add dynamical fermions. The Euclidean path integral for fermions has a probability interpretation when the temporal boundary conditions of the fermions are chosen to be anti-periodic. The fermion action (for fundamental representation fermions) explicitly breaks the $Z(N)$ symmetry, favoring the vacuum in which the Polyakov loop takes a positive value.

For the physical case of three colors, the deconfinement transition is first order for the pure gauge theory and is believed to disappear as the fermion mass is reduced from infinity, as only one vacuum configuration is energetically favored. This is all well known: for an early review, see [1].

However, if the fermions obey periodic boundary conditions, the vacuum at the positive center element is disfavored. If the number of colors is odd, there are two degenerate minima in the free energy, corresponding to complex-conjugate values of the order parameter. One of these is selected as the vacuum and thus charge conjugation is spontaneously broken. The radius of the compact dimension at which the transition from C-conserving to C-broken occurs is a physical property of QCD.

The earliest discussion of this new phase that we are aware of is by van Baal [2, 3]. He was interested in QCD with all three spatial dimensions taken to be small. In this case there are 2^3 degenerate vacua, two per small dimension. While he suggested that numerical simulations of QCD with compact dimensions might be interesting, we are aware of no follow-up studies.

Our interest in this problem was initiated from a quite different source: a discussion of the validity of the "orientifold QCD" programme of Armoni, Shifman, and Veneziano [4–6]. These authors proposed a large-N_c equivalence between $\mathcal{N}=1$ super Yang-Mills and QCD with a single fermion flavor in the symmetric or antisymmetric tensor representation. The latter theory is equivalent to one-flavor QCD for $N_c = 3$. The authors used this connection to make a successful prediction of the value of the condensate of one-flavor QCD [6, 7].

This summer, Ünsal and Yaffe [8] pointed out that a necessary condition for the non-perturbative equivalence of different theories is that global symmetries are realized in the same manner in both. They show that if the theories are considered on $\mathbb{R}^3 \times \mathcal{S}^1$ and the radius of $\mathcal{S}^1$ is chosen sufficiently small, QCD with tensor representation fermions will spontaneously break charge conjugation symmetry, while the supersymmetric theory does not. This work is a specific application of their earlier, more general studies [9–11].

Their discussion is very general: it depends only on the gauge group and on the representation of the fermions. We decided to look for the C-violating phase in numerical simulations, and to do this for a choice of parameters which was computationally the most inexpensive. Accordingly, we performed simulations with three colors and four flavors of fundamental representation dynamical fermions. We concentrate on zero-temperature simulations with one compact dimension (this is done in the simulation by taking the compact dimension much smaller than the other ones) but also briefly consider other situations: finite temperature plus one or more compact spatial dimensions. The transition is strong and easy to observe. We have not attempted to determine its order.

In the remainder of this section we outline theoretical expectations for C-odd phases, and then proceed to simulations and their results.

1.2 Weak and strong coupling

Asymptotic freedom ensures that a perturbative calculation of the effective potential for Polyakov lines becomes reliable if their length L is short enough. In this case the coupling at the scale $1/L$ is small and higher order corrections become negligible. For n_f flavors of

JHEP02(2007)022

massless Dirac fermions in the fundamental representation of SU(N) the effective potential for the Polyakov loop P is given by [8]

$$V_{\rm eff}(P) = -\frac{1}{LV}\log Z[P] = -\frac{1}{LV}\log\left[\frac{\det^{2n_f}(-D^2_{\rm fund})}{\det(-D^2_{\rm adj})}\right] , \tag{1.1}$$

where D^2 is the covariant Laplacian for a constant background field in a given representation and V denotes the volume of the non-compact dimensions. An evaluation of (1.1) proceeds exactly as in ref. [8]; the (positive) contribution to $V_{\rm eff}$ from the bosonic degrees of freedom (in a gauge where the Polyakov loop in the compact direction is $\mathrm{diag}(e^{iv_1},\ldots,e^{iv_N})$) is minimized when $v_j = v$ for all j, which forces P to be an element of the group center. For periodic/anti-periodic $(+/-)$ boundary conditions in the compact dimension one obtains

$$V^+_{\rm eff}(e^{iv}) = \frac{1}{L^4}\left[(2Nn_f - N^2)\frac{\pi^2}{45} - \frac{Nn_f}{12\pi^2}[v]^2(2\pi - [v])^2\right] , \tag{1.2}$$

$$V^-_{\rm eff}(e^{iv}) = V^+_{\rm eff}(-e^{iv}) , \tag{1.3}$$

where $[v] = v \bmod 2\pi$. The expression for periodic boundary conditions (1.2) has a unique minimum at $[v] = \pi$, while thermal boundary conditions favor a Polyakov loop on the positive real axis. The actual quantum vacuum configurations are those center elements of SU(N) closest to $v = \pi$ and $v = 0$, respectively. While $v = 0$ is always a center element, $v = \pi$ is not in the case of odd N. We thus expect a spontaneous breaking of charge conjugation for the case of periodic boundary conditions and an odd number of colors.

A few comments are in order:[1] For gauge group U(N) the phases $v = 0$ and $v = \pi$ are elements of the center and thus there is no spontaneous breaking of charge conjugation for fundamental representation fermions. This is different from the case of tensor representation fermions, which polarize the Polyakov line to a phase of $\pm\pi/2$ and thus always break charge conjugation. Moreover, for large N the vacua for fundamental representation fermions and periodic boundary conditions are separated from π only by $1/N$ effects. Thus the symmetry breaking disappears in the large N limit together with the difference between U(N) and SU(N) gauge groups and the effects of fundamental representation fermions in general.

Another calculation, by Hollowood and Naqvi [12], of the phase structure of gauge plus tensor-representation fermion theories with three small, compact spatial dimensions, shows the presence of a confinement-deconfinement transition, irrespective of the fermionic boundary conditions.

The variation on this explanation which is probably most familiar to a lattice practitioner comes from strong coupling and large mass expansions. (A probably incomplete set of early references includes [13 – 20].) Consider a lattice which is long in the thermal direction and in all but one of the spatial directions, which we denote by $\hat{x}$. There are N_x lattice spacings in the short direction. We parameterize our fermion action in a way which is suitable for a hopping parameter expansion, integrate out the fermions and then expand

[1] We thank Mithat Ünsal for pointing those out to us.

the determinant as a power series in the hopping parameter κ. At large mass, $\kappa \sim e^{-ma}$ where a is the lattice spacing. In lowest order, we find an effective action whose leading term is proportional to

$$S_{\rm eff} = \mp \kappa^{N_x} \sum_n \mathrm{Re\ Tr} P(\vec{n}) + \ldots \tag{1.4}$$

where $P(\vec{n})$ is the Polyakov line oriented in direction $\hat{x}$ and $\vec{n}$ labels all sites in the lattice with $x = 0$. The sign of the right hand side of eq. (1.4) reflects the boundary conditions of the fermions in direction $\hat{x}$: negative for anti-periodic, positive for periodic. This result is qualitatively similar to the result of the calculation of the effective potential: the effect of a short direction with anti-periodic boundary conditions is to break the center symmetry to its trivial value, while periodic boundary conditions bias the Polyakov loop toward a negative value. If -1 is an element of the center, then there is again a unique minimum; otherwise, there will be degenerate vacua.

We conclude this section with a few simple and general remarks:

- The actual location of a phase transition (the value of the critical compact radius L_c) can only be determined by a non-perturbative analysis. Its value is a fundamental property of QCD, like a hadron mass.

- As the quark mass goes to infinity, $L_c = 1/T_c$, the critical temperature for deconfinement in the quenched theory.

- As $m_q \to 0$ there is presumably a chiral symmetry restoration transition at some L_c. All of the old questions of the interplay of deconfinement and chiral symmetry breaking, such as whether there are two separate transitions, or one, are present again. Ünsal and Yaffe have pictures of proposed phase diagrams with separated transitions.

- Finally, for SU(3), the pure gauge deconfinement transition is first order. Fermions break the $Z(3)$ symmetry to $Z(2)$. A first order transition is stable under small symmetry breaking effects, so we expect the transition to persist as the quark mass is lowered from infinity. The transition might end in a second order critical point, or it might convert to a line of second order points. In either case, we expect that the second-order transition would be in the universality class of the three-dimensional Ising model.

2. Simulations

2.1 Methodology

In our simulations we employ the standard setup for dynamical fermion lattice simulations; we have three spatial dimensions with periodic boundary conditions and one time dimension with anti-periodic boundary conditions for the fermions. The geometry of $\mathbb{R}^3 \times \mathcal{S}^1$ is approximated by keeping all directions but one of the spatial ones (the $\hat{x}$ direction) large. We check this by verifying that Polyakov lines wrapping the large directions are

		finite L_x			scale setting		
label	am	N_x	N_s	β	N_t	N_s	β
F1	0.033	6	14	6.4 . . . 7.4	18	10	6.0, 6.2, 6.5
C1	0.05	4	10	5.4 . . . 6.4	18	10	5.7 . . . 6.4
F2	0.133	6	14	5.8 . . . 6.7	18	10	6.4, 6.6, 6.8
C2	0.2	4	10	5.8 . . . 6.9	18	10	6.1, 6.4, 6.7
C3	0.25	4	10	5.9 . . . 7.0	18	10	6.2, 6.5, 6.8
Q	∞	4	8	7.3 . . . 8.3	20	12	7.5, 7.8, 8.1

Table 1: Simulation parameters.

consistent with zero and show no phase preference. Note that the only difference to a finite temperature simulation is the choice of boundary conditions in the short direction.

In the present study we choose improved (unrooted, i.e. four-taste) staggered fermions as a computationally inexpensive way to do simulations with large dynamical fermion effects. We work with a state-of-the-art improved action to minimize cutoff effects. (We have also performed simulations with unimproved staggered fermions. They show similar results for a transition, but are disfavored for estimating continuum numbers.) While in principle there are many parameters one could vary (temperature, length and number of compact directions, quark mass, flavor number) we will focus on four-flavor simulations at zero temperature with one compact spatial dimension and only vary its length and the quark mass. Other choices are briefly discussed in section 3.1. We employ the Hybrid Monte Carlo algorithm from the publicly available MILC code[2] for improved staggered quarks [21 – 23] on a Symanzik gauge background.

The parameters of our simulations are summarized in table 1, where the value of β refers to the Symanzik improved gauge action. We ran 500-2000 trajectories per coupling value for the $N_x = 4$ simulations and 200-500 at $N_x = 6$. In all simulations the tadpole coefficient u_0 is fixed to a value of 0.875 for all simulations instead of determining it self-consistently at each value of β and am. In the scale setting runs we measure HYP smeared [24] Wilson loops to extract the hadronic scale r_0 [25] from the static quark potential [26] with results shown in figure 1. The solid lines are parameterizations of the form

$$\log(r_0/a) = c_0 + c_1\beta + c_2\beta^2 \,, \tag{2.1}$$

which we use to interpolate r_0. Throughout this work we will assume $r_0 = 0.5\,\mathrm{fm}$. Note that since we do not tune u_0 self-consistently, our bare action differs from the one used in ref. [27] and we therefore obtain rather different values of r_0/a as a function of β.

2.2 Results

We first want to establish that we can indeed find a set of parameters where the results from section 1.2 hold qualitatively. To this end we make a comparison: we thermalize two lattices. One has a compact spatial direction, and our initial gauge configuration was

[2] `http://www.physics.utah.edu/~detar/milc/`

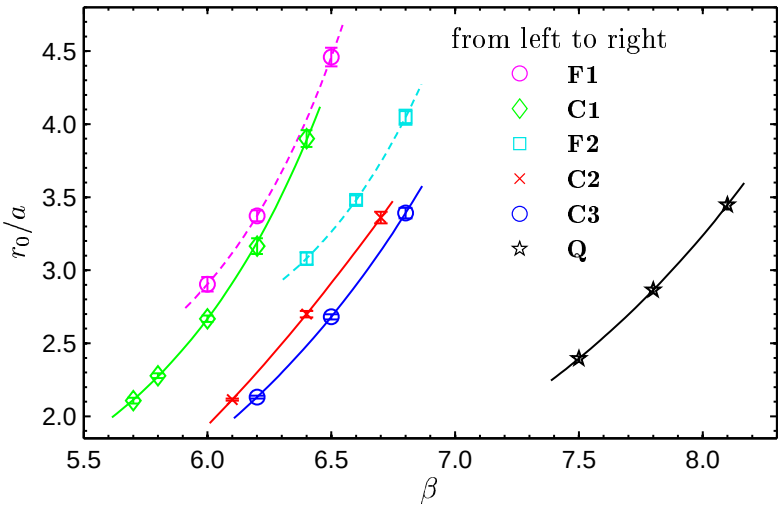

Figure 1: The hadronic scale r_0/a as a function of β in the ranges relevant for the simulations listed in table 1.

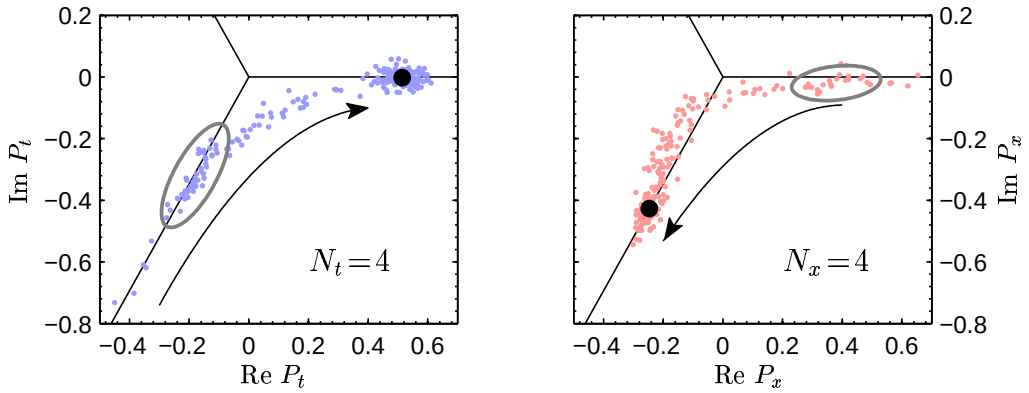

Figure 2: Thermalization histories of the Polyakov line in the short direction. Left panel: short time direction. Right panel: short spatial (x) direction.

fixed to the identity. The second configuration has a compact temporal direction, and its initial gauge fields had a time-like Polyakov loop with a phase of $\exp(-2\pi i/3)$. We choose $N_{t/x} = 4$ for the compact direction, which corresponds to $\simeq 0.6\,\mathrm{fm}$ at $\beta = 6.65$ and a quark mass of $am = 0.2$. In both cases the non-compact directions all have 10 lattice sites.

In figure 2 the direction of thermalization is indicated by an arrow for both cases. One can clearly see that the finite temperature simulation (left panel) finds a stable minimum on the real axis. The accumulation on the complex $Z(3)$ leaf (indicated by a circle) might indicate a meta-stable state. The simulation with compact *spatial* dimension (right panel) shows the opposite behavior. After following the real axis to the origin it settles to an equilibrium (indicated by a dot) with a phase around $-2\pi/3$. Thus we encounter precisely the behavior that the analytical arguments from section 1.2 suggest and now proceed to a more detailed study of the transition.

We focus on simulations with one compact spatial dimension (x) at zero temperature

JHEP02(2007)022

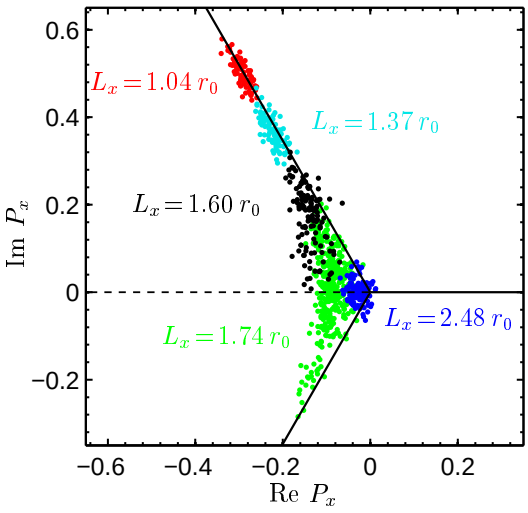

Figure 3: Equilibrium distributions of the Polyakov line from **C2** for varying extent of the compact spatial dimension.

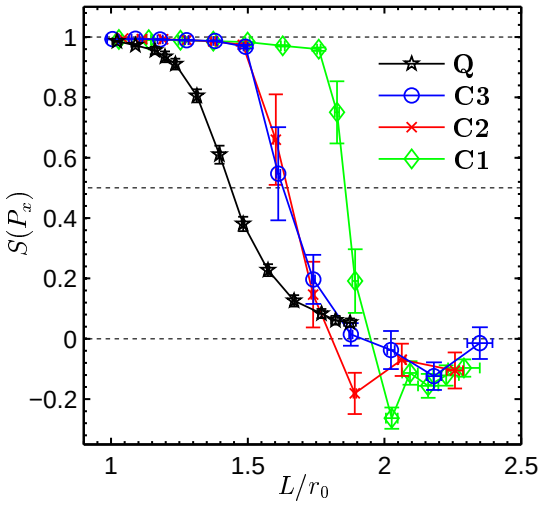

Figure 4: The observable S from eq. (2.2) for the $N_x = 4$ simulations.

and vary the extent of the compact dimension by changing β. Figure 3 shows scatter plots of P_x after equilibration from sets **C2**. For better readability each point represents the average of 5 consecutive measurements of P_x. The length of the compact dimension is indicated in units of r_0. The numerical data confirms the expectation that the fermion determinant pushes the Polyakov lines toward the negative real axis. At the largest extent we simulated with $N_x = 4$, corresponding to $L_x = 2.48\, r_0$, P_x is centered at -0.0275(17) on the real axis. With decreasing length, it moves to more negative values and spreads in the imaginary direction toward the complex center elements.

Below a certain critical length, the distribution becomes disjoint and one of the complex $Z(3)$ elements is selected as the ground state configuration with only the magnitude of P_x increasing with decreasing L_x. Thus, for SU(3) the fermion polarization spontaneously breaks charge conjugation invariance, indicated by a non-vanishing imaginary part of the Polyakov loop. With the chosen algorithm and at the volumes we simulated, no tunneling events between the two vacua were observed. This situation changes in finite temperature simulations and/or with more than one compact dimension, see section 3.1.

In principle the imaginary part of the Polyakov loop could be used to make quantitative statements about the transition. However, close to the critical length the increased spread of the Polyakov lines (see e.g. the $L_x = 1.74$ data in figure 3) would only affect the variance of the imaginary part. An observable better suited to make quantitative statements is the correlation of the phase of the Polyakov loop with that of one of the group centers $e^{2k\pi i/3}$. Another advantage is that, unlike the imaginary part, the phase of the Polyakov line does not require renormalization. We map the phase range between two SU(3) center elements to the full circle by taking $(P/|P|)^3$ and then project onto the real axis,

$$S(P) = \mathrm{Re}(P/|P|)^3 = \cos(3 \arg P) \; . \tag{2.2}$$

JHEP02(2007)022

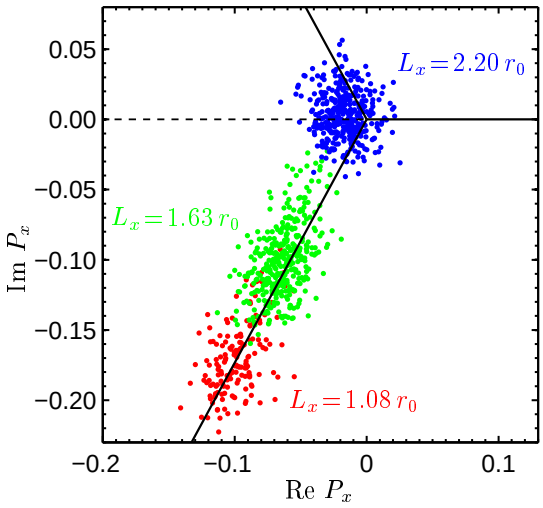

Figure 5: Equilibrium distributions of the Polyakov line from **F2**.

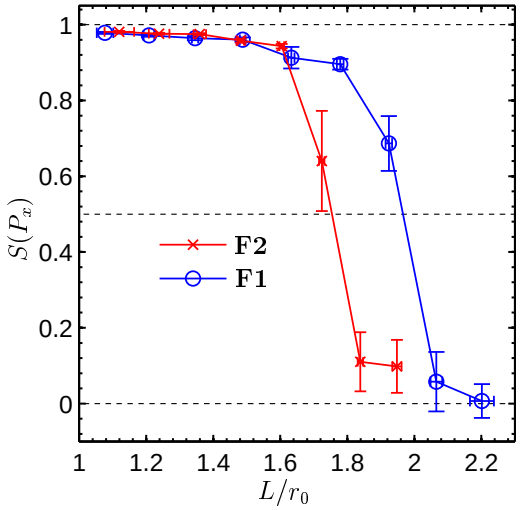

Figure 6: The center correlation S from eq. (2.2) for the $N_x = 6$ simulations.

The expectation value of $S(P)$ is close to one in the broken phase, when all Polyakov lines are in the vicinity of one of the $Z(3)$ centers. It is zero for randomly distributed phases and negative if the phases lie between the $Z(3)$ elements, e.g. around the negative real axis. (This observable is reminiscent of a similar one used to locate the pure gauge transition [28].) The center correlation $S(P_x)$ for the $N_x = 4$ simulations is shown in figure 4 as a function of the length of the compact dimension. For the dynamical simulations we observe that the value of S abruptly decreases from almost unity to small negative values before approaching zero in the large volume limit. For the heavier data sets **C3** and **C2**, the transition occurs at $\simeq 0.8\,\mathrm{fm}$ and for the lightest set **C1** with $am = 0.05$ the critical length is slightly larger at 0.93 fm. The extraction of the critical length is discussed in the next section.

For comparison we also show the quenched results, run **Q**. As discussed above, the quenched limit of our setup is just the familiar finite temperature phase transition for the pure gauge theory. Here the behavior is qualitatively different as all *three* center elements are equivalent vacua in the broken phase. Moreover, the heatbath/overrelaxation algorithm allows tunneling between those. With our chosen observable the transition appears much smoother than in the presence of dynamical fermions.

To establish that we are indeed seeing a *physical* effect and not just lattice artifacts, we simulated finer lattices ($N_x = 6$). Data from the $N_x = 6$ simulations are shown in figures 5 and 6.

The results from the finer lattice spacing are qualitatively similar to the $N_x = 4$ data presented in figures 3 and 4. The transition is still present and only slightly more rounded. The critical length has moved to somewhat larger values and there is no longer a region of negative values of $S(P_x)$ just above the transition. One might thus interpret this behavior as a lattice artifact that disappears when going from $N_x = 4$ to 6.

JHEP02(2007)022

label	am	N_x	β_c	$L_c/\,\mathrm{fm}$	$L_c^{-1}/\,\mathrm{MeV}$
F1	0.033	6	6.070(12)	0.983(14)	201(9)
C1	0.05	4	5.728(9)	0.928(9)	213(4)
F2	0.133	6	6.574(20)	0.877(14)	225(12)
C2	0.2	4	6.269(25)	0.822(17)	240(12)
C3	0.25	4	6.387(34)	0.814(22)	242(16)
Q	∞	4	7.752(11)	0.719(6)	274(6)

Table 2: Results for the critical length.

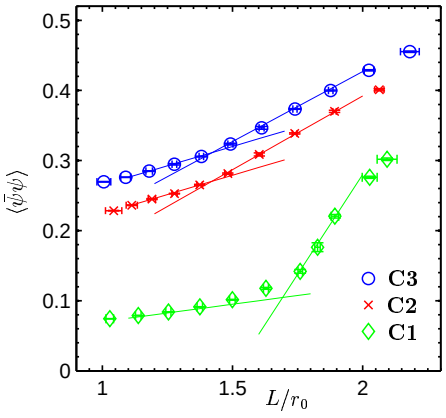

Figure 7: The scalar condensate $\langle\bar{\psi}\psi\rangle$ vs. the extent of the compact dimension for the $N_x = 4$ runs.

Finally, we consider the chiral condensate $\langle\bar{\psi}\psi\rangle$. A non-vanishing expectation value indicates spontaneous breaking of chiral symmetry, which occurs in large volumes. Finite volume, non-zero quark mass as well as discretization errors tend to wash out this transition such that only a smooth crossover is observed. As we are only interested in the qualitative behavior across the transition, we consider the unrenormalized lattice condensate. The results from the $N_x = 4$ runs, again as a function of L/r_0, are shown in figure 7. As expected, for the heavier masses (**C2**, **C3**) no strong signal is observed. However, as marked by the lines, there is an inflection point, where the slope (as a function of L_x) increases as the compact dimension gets bigger. The former is located just below $L = 1.5\, r_0$, which is where the center correlation (see figure 4) starts to drop. The lightest mass (**C1**) shows a much stronger crossover and again the inflection point agrees with the data from the center correlation. Almost identical results are obtained at the finer lattices.

Thus the data indicate that in $N_f = 4$ QCD, at zero temperature with one compact spatial dimension, there is a single crossover, i.e. a critical length, below which chiral symmetry is restored and charge conjugation is spontaneously broken.

3. Interpretation

As a definition of the critical coupling β_c we take the value, where the center correlation $S(P) = 0.5$. In practice we linearly interpolate between the two values of β above and below this point. Since this quantity shows a sharp transition the results will not change significantly when different definitions are adopted. The values of β_c and the critical length L_c for all runs are given in table 2. The error on L_c includes the (statistically independent) error of r_0.

Taking into account the rather coarse lattice spacing and the arbitrariness in the precise definition of the critical length, the result for the quenched case is in good agreement

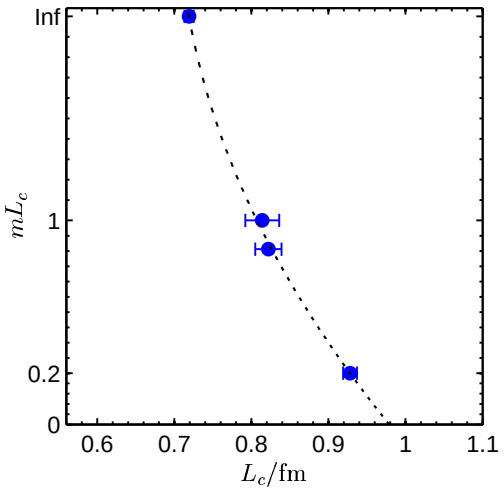

Figure 8: The phase diagram at $N_x = 4$, where we have three dynamical and a quenched data point for the critical length of the compact dimension.

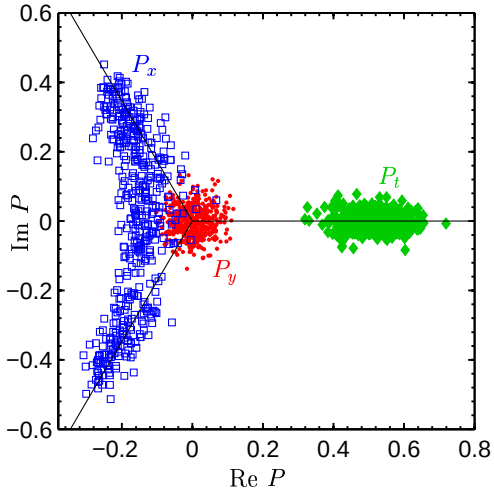

Figure 9: Equilibrated Polyakov lines for $\beta = 6.65$, $am = 0.2$ and $[N_x, N_y, N_z, N_t] = [4, 10, 10, 4]$.

with other determinations of the quenched critical temperature (see e.g. [29], who quotes $T_c \sim 270\,\mathrm{MeV}$.) Comparing the data from the coarse dynamical lattices in table 2 we see that the critical length increases with decreasing quark mass. Data at fixed $N_x \cdot am = mL_c$, i.e. **C1**/**F1** and **C2**/**F2**, suggest that scaling violations are not large and that the lattice artifacts decrease the value of L_c. An extrapolation assuming a^2 scaling gives continuum values of $L_c = 1.027(26)\,\mathrm{fm}$ and $0.922(29)\,\mathrm{fm}$ for $mL_c = 0.2$ and 0.8, respectively.

Using all the $N_x = 4$ data, we obtain a phase diagram of the critical length as a function of the quark mass as shown in figure 8. The critical length increases as the quark mass is lowered from infinity and although we have no data at very light quark masses, the dependence does not seem to be very strong. Clearly, more quantitative statements will require simulations at finer lattice spacing and more (and lighter) quark masses.

3.1 Other geometries

To briefly explore other geometries, we chose a parameter set in the broken phase ($am = 0.2$, $\beta = 6.65$) and simulated all possible combinations of compact ($N = 4$) and non-compact ($N = 10$) dimensions, including finite temperature. In all cases we confirm our expectation that compact spatial dimensions support a Polyakov loop in one of the two complex $Z(3)$ directions while a compact time direction produces a positive Polyakov loop. If more than one spatial dimension is short, the bulk volume is reduced and we observe tunneling between the two states. The values of the Polyakov loops in the compact direction are not correlated, showing that indeed all vacua are equivalent.

At finite temperature already one spatial dimension allows tunneling of the Polyakov line in the compact space dimension. figure 9 shows Polyakov lines from such a geometry. While those from the non-compact dimensions cluster around zero (P_y; P_z not shown) the time-like loops have a positive mean value and those in the compact spatial dimensions

JHEP02(2007)022

spread along the complex $Z(3)$ directions. It is not known whether the transition persists at high temperature and whether the finite temperature transition at $1/L_x = 0$ and the C breaking transition at zero temperature are connected. However, an exploration of the phase diagram of inverse temperature and compact length might be interesting.

4. Summary

For the usual kind of QCD simulations, where the goal is to model QCD in infinite volume, the C-breaking transition is just an artifact which needs to be checked. For example, Ünsal and Yaffe commented that our study of the $N_f = 1$ condensate might have been done in the C-broken phase. We checked our data sets for our studies of the $N_f = 1$ and 2 condensates [7, 30] and verified that we were in the C-symmetric phase.

In the present paper we studied QCD with dynamical quarks with one compact spatial dimension. We find a fundamental length scale, the critical length L_c, below which QCD with four dynamical quark flavors shows spontaneous breaking of charge conjugation. The continuum value of L_c is approximately 1 fm. It seems to be connected to the finite temperature transition in the limit of infinite quark and persists down to the smallest quark masses we simulated. There we also observe a crossover in the chiral condensate, signaling the restoration at chiral symmetry at the same critical length. We have not determined the order of the transition: this would require more extensive finite-size scaling studies.

The spontaneous breaking of charge conjugation is expected from both perturbative arguments and a strong coupling expansion. For technical reasons we performed simulations with four quark flavors but do not expect the conclusions to change significantly for other choices. (We have done some pilot studies with $N_f = 2$ flavors of improved Wilson fermions, and have also seen the crossover to a C-broken phase.) Clearly we are seeing only the tip of the iceberg: just as for the finite-temperature transition, the transition is affected by the number of colors and flavors, group representation of the fermions, and the relative sizes of all small compact dimensions.

Acknowledgments

We are grateful to Mithat Ünsal and Larry Yaffe for correspondence which initiated this investigation, and to Mithat Ünsal for a critical reading of the manuscript. Some of the simulations were performed on the cluster at Fermilab. This work was supported in part by the US Department of Energy.

References

[1] B. Svetitsky, *Symmetry aspects of finite temperature confinement transitions*, *Phys. Rept.* **132** (1986) 1.

[2] P. van Baal, *The small volume expansion of gauge theories coupled to massless fermions*, *Nucl. Phys.* **B 307** (1988) 274.

[3] P. van Baal, *QCD in a finite volume*, `hep-ph/0008206`.

[4] A. Armoni, M. Shifman and G. Veneziano, *Exact results in non-supersymmetric large-N orientifold field theories*, *Nucl. Phys.* **B 667** (2003) 170 [hep-th/0302163].

[5] A. Armoni, M. Shifman and G. Veneziano, *SUSY relics in one-flavor QCD from a new 1/N expansion*, *Phys. Rev. Lett.* **91** (2003) 191601 [hep-th/0307097].

[6] A. Armoni, M. Shifman and G. Veneziano, *QCD quark condensate from SUSY and the orientifold large-N expansion*, *Phys. Lett.* **B 579** (2004) 384 [hep-th/0309013].

[7] T. DeGrand, R. Hoffmann, S. Schaefer and Z. Liu, *Quark condensate in one-flavor QCD*, *Phys. Rev.* **D 74** (2006) 054501 [hep-th/0605147].

[8] M. Ünsal and L.G. Yaffe, *(In)validity of large-N orientifold equivalence*, *Phys. Rev.* **D 74** (2006) 105019 [hep-th/0608180].

[9] P. Kovtun, M. Unsal and L.G. Yaffe, *Non-perturbative equivalences among large-N_c gauge theories with adjoint and bifundamental matter fields*, *JHEP* **12** (2003) 034 [hep-th/0311098].

[10] P. Kovtun, M. Unsal and L.G. Yaffe, *Necessary and sufficient conditions for non-perturbative equivalences of large-N_c orbifold gauge theories*, *JHEP* **07** (2005) 008 [hep-th/0411177].

[11] P. Kovtun, M. Unsal and L.G. Yaffe, *Can large-N_c equivalence between supersymmetric Yang-Mills theory and its orbifold projections be valid?*, *Phys. Rev.* **D 72** (2005) 105006 [hep-th/0505075].

[12] T.J. Hollowood and A. Naqvi, *Phase transitions of orientifold gauge theories at large-N in finite volume*, hep-th/0609203.

[13] T. Banks and A. Ukawa, *Deconfining and chiral phase transitions in quantum chromodynamics at finite temperature*, *Nucl. Phys.* **B 225** (1983) 145.

[14] M. Ogilvie, *An effective spin model for finite temperature QCD*, *Phys. Rev. Lett.* **52** (1984) 1369.

[15] J. Bartholomew, D. Hochberg, P.H. Damgaard and M. Gross, *Effect of quarks on* SU(N) *deconfinement phase transitions*, *Phys. Lett.* **B 133** (1983) 218.

[16] F. Green and F. Karsch, *Mean field analysis of* SU(N) *deconfining transitions in the presence of dynamical quarks*, *Nucl. Phys.* **B 238** (1984) 297.

[17] P. Hasenfratz, F. Karsch and I.O. Stamatescu, *The* SU(3) *deconfinement phase transition in the presence of quarks*, *Phys. Lett.* **B 133** (1983) 221.

[18] T.A. DeGrand and C.E. DeTar, *Phase structure of QCD at high temperature with massive quarks and finite quark density: a Z(3) paradigm*, *Nucl. Phys.* **B 225** (1983) 590.

[19] A. Gocksch and M. Ogilvie, *Finite temperature deconfinement and chiral symmetry restoration at strong coupling*, *Phys. Rev.* **D 31** (1985) 877.

[20] F. Green and F. Karsch, *The* SU(4) *deconfining transition at strong coupling: a Monte Carlo study*, *Phys. Rev.* **D 29** (1984) 2986.

[21] MILC collaboration, K. Orginos, D. Toussaint and R.L. Sugar, *Variants of fattening and flavor symmetry restoration*, *Phys. Rev.* **D 60** (1999) 054503 [hep-lat/9903032].

[22] C.W. Bernard et al., *The QCD spectrum with three quark flavors*, *Phys. Rev.* **D 64** (2001) 054506 [hep-lat/0104002].

JHEP02(2007)022

[23] C. Aubin et al., *Light hadrons with improved staggered quarks: approaching the continuum limit*, *Phys. Rev.* **D 70** (2004) 094505 [hep-lat/0402030].

[24] A. Hasenfratz and F. Knechtli, *Flavor symmetry and the static potential with hypercubic blocking*, *Phys. Rev.* **D 64** (2001) 034504 [hep-lat/0103029].

[25] R. Sommer, *A new way to set the energy scale in lattice gauge theories and its applications to the static force and alpha-s in* SU(2) *Yang-Mills theory*, *Nucl. Phys.* **B 411** (1994) 839 [hep-lat/9310022].

[26] A. Hasenfratz, R. Hoffmann and F. Knechtli, *The static potential with hypercubic blocking*, *Nucl. Phys.* **106** *(Proc. Suppl.)* (2002) 418 [hep-lat/0110168].

[27] C. Gattringer, R. Hoffmann and S. Schaefer, *Setting the scale for the Luescher-Weisz action*, *Phys. Rev.* **D 65** (2002) 094503 [hep-lat/0112024].

[28] N.H. Christ and A.E. Terrano, *The deconfining phase transition in lattice QCD*, *Phys. Rev. Lett.* **56** (1986) 111.

[29] F. Karsch, *Lattice QCD at finite temperature and density*, *Nucl. Phys.* **83** *(Proc. Suppl.)* (2000) 14 [hep-lat/9909006].

[30] T. DeGrand, Z. Liu and S. Schaefer, *Quark condensate in two-flavor QCD*, *Phys. Rev.* **D 74** (2006) 094504 [hep-lat/0608019].

JHEP02(2007)022